Some Tribological Influences on the Electrode-Worksheet Interface During Resistance Spot Welding of Aluminum Alloys

M. Rashid

(Submitted April 20, 2010)

In this study, the effect of worksheet surface characteristics on the electrical contact resistance of electrode-worksheet interface during resistance spot welding of aluminum alloy (AA5182) was discussed. The electrical contact resistance was influenced by both the oxide layer and surface roughness of the worksheet. However, the effect of oxide layer was more dominant, and the effect of surface roughness was likely to be linked with the damaging of oxide layer and not the contact area. The oxide layer on AA5182 was non-uniform with Mg-rich small spots dispersed on the surface. Grinding and scratching the worksheet surface was effective in reducing the oxide layer thickness and, hence, reduced the electrical contact resistance. It was observed that the surfaces with higher electrical contact resistances at this interface showed faster pitting rate of electrode. The study also suggested that the static electrical contact resistance measured before resistance spot welding could be useful for predicting materials likely behavior during the actual resistance spot welding process of AA5182.

1. Introduction

With good formability and strength-to-weight ratio, 5xxx series aluminum alloy sheets are generally considered for autobody inner panel and frames (Ref 1, 2). For most sheet metal applications, resistance spot welding (RSW) remains the main choice. The RSW process is fast, does not require high-skilled labor, and can easily be automated and is very popular in the automotive industry (Ref 1, 2). Depending on the size of the vehicle, an autobody can have spot weld joints in the range of 7000-12000 (Ref 3). However, welding of aluminum alloys remains a challenge. The main problems are the short electrode tip life and inconsistent weld quality during continuous RSW of aluminum alloys (Ref 4-6).

The reason for these problems is ascribed to electrode pitting which, for a given set of welding condition, is the most influential characteristic on nugget quality and joint strength (Ref 4, 5, 7, 8). Unlike steel, the main source of heat during RSW of aluminum alloys is the electrical contact resistance at the interfaces, but not the bulk resistance of the worksheet (Ref 8-10). This heat generation is essential at the sheet-sheet interface or faying surface (FS) and provides the joule heating for nugget formation. However, the electrical contact resistance

at the electrode-worksheet (E/W) interface caused local alloying of electrode and worksheet material which ultimately resulted in electrode pitting and, thus reducing the useful life of the electrode as well as causing deterioration in the joint quality during continuous RSW of aluminum alloys (Ref 4, 5, 10); therefore, the electrical contact resistance at the interfaces is the most significant variable in RSW of aluminum alloys. This electrical contact resistance depends heavily on the tribological characteristics of the contacts at the two interfaces (FS and E/W). The most influential tribological features of aluminum work sheets are the presence of an oxide layer, surface roughness, and the presence of a chemical or lubricant. Numerous studies (Ref 8, 9, 11, 12) have been conducted to understand the influence of each of these characteristics, among which oxide layer was found to be the most influential. Although surface roughness was influential on the amount of electrical contact resistance, it was also attributed mainly to disturb and damage the surface oxide layer. Further, the presence of chemicals or lubricants was found (Ref 5, 6, 13) to alter the contact resistance at the interfaces and hence modify the outcome of the RSW of aluminum alloys.

Depending on the processing condition, the surface oxide layer of aluminum alloys may not be uniform, and other oxides like MgO could also be present along with alumina (Al_2O_3) (Ref 14, 15). Both alumina (Al_2O_3) and magnesia (MgO) act as electrical insulators (Ref 16), and current flow through the interfaces (FS and E/W) is only possible due to the cracks in this layer which allows establishing a metal-to-metal contact at these interfaces (Ref 17). Patrick et al. (Ref 14) attributed this cracking of the hard brittle oxide layer to the deformation at the asperity tips but no details were available about the local contact stress and bending stress that would have developed in the oxide layer. Although these metal-to-metal contacts are good for electrical conductivity, these contacts are very small in size and few in numbers (Ref 12). During the passage of high

M. Rashid, CANMET, Materials Technology Laboratory, Natural Resources Canada, 568 Booth Street, Ottawa, ON K1A 0G1, Canada; and Department of Mechanical and Mechatronics Engineering, University of Waterloo, Waterloo, ON N2L 3G1, Canada. Contact e-mail: murashid@nrcan.gc.ca.

weld current through these small contacts, the current density becomes very high and causes constriction resistance (Ref 9, 12, 13). On the as-received aluminum worksheet, the oxide layer could be very thick, and electrical contact resistance would only be consisted of constriction resistance (Ref 8, 12, 14, 18, 19).

In this study, a direct comparison of the as-received surface with that of the abraded and ground surfaces was established. The objective was to characterize the main features of the AA5182 worksheet surface and their influence on electrode life. The focus was the worksheet surface at the E/W interface. All these surfaces were analyzed for electrical contact resistance (static) at the E/W interface while RSW was also performed on some surfaces to understand the pitting behavior. This study also discussed the possibility of using static electrical contact resistance as an indicator of welding behavior of AA5182.

2. Materials and Methods

Worksheet of aluminum alloy 5182 (AA5182) of thickness 1.5 mm was used for the entire studies (Table 1). Different surface treatments were performed only on one side of the mill-finished worksheet surfaces to prepare different surface characteristics associated with the E/W interface. The intent was to investigate the variability of the E/W interface only. All welding was performed using a 170-kVA medium frequency direct current (MFDC) spot welder (pedestal type) made by Centerline Limited, Windsor, Canada. Welding parameters (Table 2) for this study were selected based on the preliminary investigation on the same material. Class-I type copper-0.15% zirconium electrodes (Ref 20) were used for these experiments. Theses electrodes were truncated type (taper angle 60°) with a spherical tip of face diameter 10 mm and radius of curvature 50 mm.

2.1 Set 1: Electrical Contact Resistance Experiment

These experiments were designed to investigate the effect of surface characteristics (roughness and oxide layer) on the electrical contact resistance of the E/W interface. Two roughness levels higher and lower than the as-received condition were obtained. Specimens were cut in the size of 50 mm × 40 mm and then grinding (in the rolling direction) was performed manually with two different grades of silicon carbide papers. The centerline average surface roughness (R_a) was recorded with a direct contact profile meter (Surtronic +3,

Table 1 Different alloying elements in AA5182

Element	Mg	Mn	Fe	Si	Cu	Cr	Zn	Ti	Al
wt.%	4.71	0.32	0.19	0.08	0.05	0.01	0.01	0.02	Bal

Table 2 Weld schedule and welding parameters for RSW (1 cycle = 16.67 ms)

Weld schedule		Welding parameter	
Squeeze	25 cycles	Weld force	6 kN
Current	5 cycles	Weld current	29 kA
Hold	12 cycles	Weld rate	20 spots/min

Taylor Hobson Ltd, Leicester, UK). Three measurements were recorded on each specimen, and the average of them was reported as the R_a value for that specimen. Five such specimens were used for each surface condition, and the overall average of these specimens gave the characteristic R_a for the particular surface preparation.

Same specimens were used to measure the electrical contact resistances (static) at the E/W interface employing the four-point method (Ref 8) (Fig. 1). Spot welder was used to clamp the specimens between electrodes using the same force (6 kN) as for weld. Resistances were recorded at room temperature by measuring the voltage drop across terminals (P_1 and P_2) while passing a 10-A current through electrodes (C_1 and C_2) using a digital low-resistance ohmmeter (DLRO-10X, AVO International, Scunthorpe, UK). The contact zone of the worksheet surface was carefully selected to avoid regions where the direct contact profilometer had touched it for roughness measurement as it could influence the results. In order to avoid any variability of the electrode tip surface, the same pair of electrodes was used for all these specimens. Furthermore, through preliminary experiments, it was observed that the static electrical contact resistance remained same after the first 10-20 measurements (Ref 11) and therefore, 20 conditioning measurements (static) were performed with the pair of electrodes before using them for the actual measurement of the above mentioned specimens.

2.2 Set 2: Electrode Pitting Experiments

The intent of these experiments was to investigate the effect of grinding on the electrode degradation behavior and joint shear strength. Specimens of only one type of ground surface were compared with the as-received surface. Since a large number of samples were required, the grinding was performed with the help of rotating wheel of scotch-brite. Samples were held against the rotating wheel, and grinding was performed along the rolling directions. This type of ground surface is designated hereafter as "abraded" surface, in this study. Also, it was intended to keep the R_a value of these abraded samples as close to that of the as-received surface as possible to investigate the effect of grinding only.

For every surface condition, 100 spot welds were performed, and each set of 100 spot welds was divided into four stages. Each stage consisted of taking carbon imprints of the electrode at zero current, followed by 5 spot welds on overlapped (shear test) specimens (Fig. 2), and then 20 spot welds (10 each) on standard welding coupons. After stage 4, carbon imprints were taken, and finally, five overlapped specimens were welded. For each surface condition, a fresh
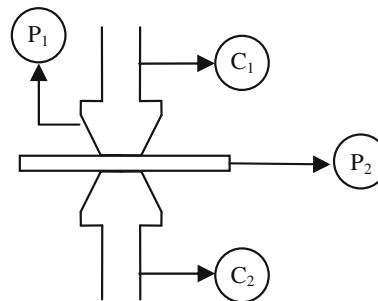
Fig. 1 Schematic illustration of four-point method for electrical contact resistance measurement

pair of electrode was used, and conditioning of electrodes was performed using the standard procedure before actual spot welding. For comparison, the center line average roughness (R_a) and the electrical contact resistance (static) of the E/W interface were also measured for both these surface conditions.

2.3 Testing and Metallography

Shear test of spot-welded specimens were performed using Instron tensile testing machine (Model-4206, Canton, MA). Optical/stereo microscopy was used for general observations at different magnifications. For high resolution images and chemical analysis of both electrode and worksheet surfaces, scanning electron microscope (SEM) and electron dispersion x-ray spectroscopy (EDX) were performed using Jeol electron microscope. These devices were part of a SEM facility (model JSM-840 manufactured by JEOL USA, Inc) that operated at 20 kV.

3. Results

3.1 Electrical Contact Resistance

The as-received AA5182 surface had a centerline average surface roughness (R_a) value of 0.32 μm. The manual grinding of sheet surface with different grades of silicone carbide papers produced samples with R_a values above and below those of the as-received surface (Table 3). A statistical analysis (one-way ANOVA) indicated that there were significant differences between the R_a values for the three different surface conditions ($p < 0.001$). This indicated that these samples were from three different roughness groups.

The sheet surface roughness associated with the E/W interface had a very clear effect on the static electrical contact resistance at this interface (Fig. 3). Among the ground surfaces, smooth surfaces showed higher average contact resistance (9.1 μΩ) than the rough surfaces (7.2 μΩ). James et al. (Ref 8) performed similar electrical resistance measurements with the same load on 2.0-mm-thick abraded AA5754 sheet
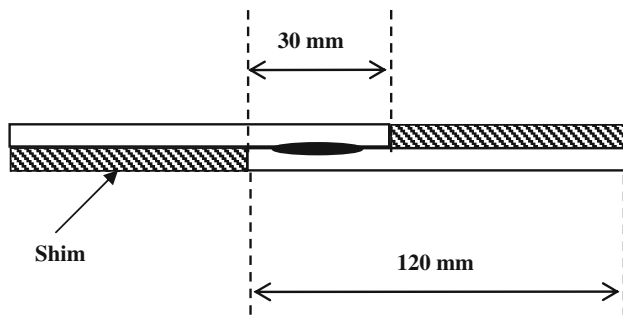
($R_a = 0.76$ μm) and reported the static electrical contact resistance values of the ground surfaces in the range of 10-12 μΩ, which were found to be in quite good agreement with those of this study. However, the effect of roughness levels observed for ground surfaces was not consistent with the as-received surface. Although, the as-received sheet surface had a roughness level in between the rough and smooth levels, the average electrical contact resistance of the as-received surface (11.6 μΩ) was higher than both the ground surfaces.

These results clearly suggested that the surface roughness was not the only variable controlling the electrical contact resistance of the E/W interface, but the geometry of the oxide layer present at the surface was also having very significant effect. Even for the ground surfaces, the trend shown above for the roughness was not expected. If the contact involved predominantly elastic deformation, then the real area of contact would be lower for the rough surface and thus electrical contact resistance would be higher. However, if the contact involved predominantly plastic deformation, then the real contact area would approach the nominal one (Ref 21), and the electrical contact resistance would be independent of surface roughness. Thus, the resulting higher electrical contact resistance for the smoother surface suggested that there was some other influencing factor. Statistical analysis indicated that there were significant differences between the electrical contact resistance values for the three different surface conditions ($p < 0.001$). This finding was almost certainly a consequence of a more thick oxide layer on the as-received surface whereas both the ground specimens (rough and smooth) had their oxide layer damaged to varying extents by the grinding process thus reducing its insulating effect.

3.2 Electrode Pitting

The results of Set-2 experiments were consistent with those of Set-1 experiments (Table 4). Although the electrical contact

Fig. 2 Configuration of the overlapped shear test specimens
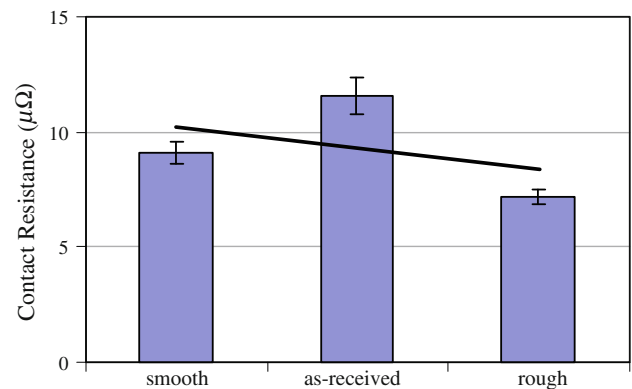
Fig. 3 Electrical contact resistance (static) at the E/W interface for as-received and ground surfaces

Table 3   Centerline average roughness (R_a) of the contacting surface of the worksheet

Surface	No. of specimens	Total no. of roughness measurements	Preparation method	R_a, μm Avg. ± SD
Smooth	5	15	Grinding with 600 Grade silicon carbide paper	0.24 ± 0.02
As-received	5	15	None	0.32 ± 0.02
Rough	5	15	Grinding with 180 Grade silicon carbide paper	1.08 ± 0.06

Table 4 R_a values and electrical contact resistance of as-received and abraded surfaces (average of 20 measurements)

Surface	R_a, μm Avg. ± SD	Electrical contact resistance, μΩ Avg. ± SD
As-received	0.33 ± 0.05	16.3 ± 3.0
Abraded	0.39 ± 0.04	13.9 ± 2.9

Surface Condition	Positive Electrode		Start of pitting	Contact area growth (%)
	Start	**After 100 RSW**		
as-received			25 -50 spots	26
abraded			50 -75 spots	17
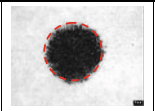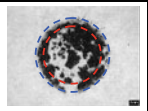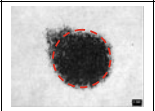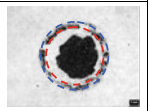
Fig. 4 Carbon imprints showing the electrode pitting behavior for different surfaces; dotted circles show initial (inner) and final (outer) contact diameter

resistance had a sample-to-sample variation which was similar to that found by other investigators (Ref 13, 19), within one set of experiments, in which measurements were obtained with the same pair of electrodes and samples were prepared from the same sheet, the results were consistent with resistance had much less scatter. Although the average R_a of the as-received surfaces (0.33 μm) was not much less than that of the abraded surfaces (0.39 μm), it still caused a fairly large drop in the electrical contact resistance from 16.3 to 13.9 μΩ, respectively ($p = 0.01$).

Results from the welding experiments also showed very clear effect of abrading on the pitting behavior of electrodes (Fig. 4). The as-received surface that had a higher electrical contact resistance showed different pitting behavior than that of abraded surface. The pitting was more extensive, and it started earlier for the as-received surfaces than for the abraded surfaces. It was considered likely that the higher electrical contact resistance of the E/W interface associated with the as-received surface caused more heat generation at this interface and hence more alloying, pickup, and pitting of electrode. This finding was also supported by the growth of the contact area between electrode and worksheet. It was observed that, for both these surfaces, there was hardly any change in the contact area before the start of pitting. However, the contact area growth between electrode and worksheet for as-received surface was much higher than the abraded surfaces.

Abrading the contacting surface of the worksheet associated with the E/W interface also resulted in a slightly decrease of the initial joint shear force of the welds compared with the as-received surfaces (Fig. 5). All these results followed the usual trend of electrode life (Ref 4, 5) in that the joint strength increased initially to reach a peak value and then started decreasing. Although the initial joint shear force of abraded sheet was slightly lower than that of as-received surface, it was still well above the acceptable joint shear force of this material (Ref 22). Furthermore, with continuous welding, the difference
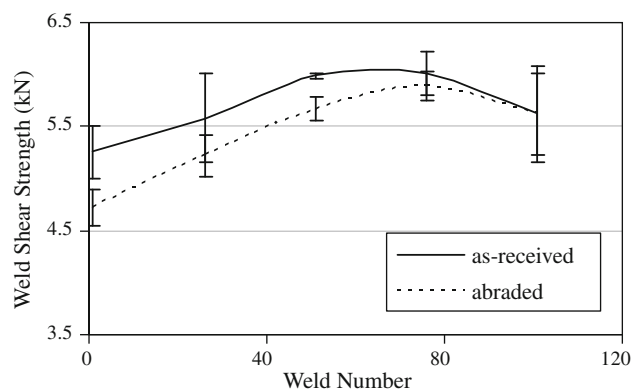
Fig. 5 Joint shear force comparisons for as-received and abraded surfaces

of joint shear strength of these surfaces decreased and reached the same value at the end of 100 spot welds. At that stage, from these results, it was not clear as regards which surface would provide better electrode life. However, the faster pitting rate of electrode associated with as-received surface could be suggesting an early failure of the electrode.

4. Discussion

The theory of tribology (Ref 21) suggests that in case of elastic or elastic/plastic contact between the two mating surfaces, the real area of contact is always less than the apparent area of contact. However, if the deformation is fully plastic, then the real area of contact approaches the apparent area of contact. Thus, the first step in any technical discussion of the tribology of the E/W interface must begin with a determination of the extent of plastic deformation. Also, it must be recognized that the oxide layer on the aluminum worksheet surface has a higher elastic modulus than the substrate and acts as an electric insulator. As a result, it may influence surface deformation and electrical resistance (Ref 9). In this study, all other factors were kept constant, and only the contacting surfaces of the worksheet associated with the E/W interface were ground or abraded to determine the effects on electrical contact resistance and weld shear strength.

4.1 Effect of Surface Roughness

Initially and in accordance with the literature (Ref 21), it was thought that surface roughness at the E/W interface would influence the effective electrode life because the real area of contact would decrease with increasing surface roughness, and thus the electrical contact resistance would *increase*. However, for ground surfaces, the electrical contact resistance decreased with increasing surface roughness, and this might have been a consequence of plastic deformation making the real and apparent areas of contact equal; the drop in resistance could be related to damage of the oxide layer on the aluminum caused by the grinding/abrading process and/or the more extensive bending/cracking of the oxide layer that re-formed on the rougher surface when the substrate sustained extensive plastic deformation.

The first step then was to estimate the extent of plastic deformation using the elastic properties of the surfaces

(aluminum worksheet and copper electrode) along with the surface geometry. Hertzian contact equations were employed to calculate the average contact stress (σ_{avg}) assuming pure elastic deformation and perfectly smooth surfaces. The resulting value of the Hertzian contact stress (σ_{avg}) was 716.1 MPa and since this value was almost equal to the hardness of the aluminum surface (784.8 MPa) as measured with a Vickers indenter (50 gf), extensive plastic deformation was expected reaching almost to the surface. This value of the average Hertzian contact stress was much higher than the $3\sigma_y$ of the worksheet material (414 MPa) which is also considered as a criterion for plastic deformation. It was interesting to note that the Vickers hardness values increased when the test was performed with lower loads because the oxide layer, although thin, had much higher hardness than the bulk aluminum (Ref 17). Thus, it was not entirely clear what hardness was appropriate for estimating the extent of plastic deformation in the above comparison with the average Hertzian contact stress. It was considered likely that a lower value would be more appropriate, and if so, the plastic deformation would be more extensive.

For a contact with extensive plastic deformation, the real and apparent contact areas would be virtually identical. Thus the only link between the electrical contact resistance and surface roughness was likely to be related to how the oxide layer was deformed in the contact. The rougher surface might subject the oxide layer to deform more during the plastic deformation of the aluminum substrate and thus promote oxide layer cracking with a reduction in electrical contact resistance. Alternatively, the more extensive grinding/abrading process performed on the rougher surface might have damaged the oxide layer leading to a drop in contact resistance. In either case, the oxide layer geometry during the RSW process was an important consideration as to be subsequently discussed.

4.2 Oxide Layer on AA5182

For its high affinity of oxygen, an oxide layer is always present at the aluminum surface and will quickly reform if disturbed chemically or mechanically. Depending on the processing/storage condition, other oxides such as MgO could also be present on the as-received surface (Ref 14, 23). This was consistent with the results where the electrical contact resistance of the as-received surface was higher than the ground and abraded surfaces. All those ground surfaces were prepared within 2 h of experiments and were expected to have fresh, thin, and uniform oxide layer (Ref 8) while the as-received surface was untreated and would have thicker perhaps less uniform oxide layers.

The Mg content on the polished and as-received surfaces of AA5182 was 4.6 and 4.7%, respectively; these values were very close to the nominal value of 4.5%, often given for this aluminum alloy (AA5182), and the 4.7% value provided by the manufacturer. However, for the as-received surface, the Mg content was not uniform over the entire surface. SEM micrographs showed that there were several spots on the surfaces which were not consistent with the general surface morphology and appeared bright in contrast (Fig. 6). Chemical analysis (EDX) of those spots revealed different chemistry than the general surface area. These bright spots appeared richer in magnesium and oxygen (Fig. 6, Sp-1 and Sp-2) while the dark portion of the surface had less Mg content than the alloy composition (Fig. 6, Sp-3, Sp-4, and Sp-5). Additional continuous chemical analysis (line scan EDX) across such

Wt %	Sp-1	Sp-2	Sp-3	Sp-4	Sp-5
Al	88.3	88.2	96.0	94.8	96.2
Mg	6.4	5.5	3.8	3.9	3.5
O	5.3	6.3	0.2	1.3	0.3
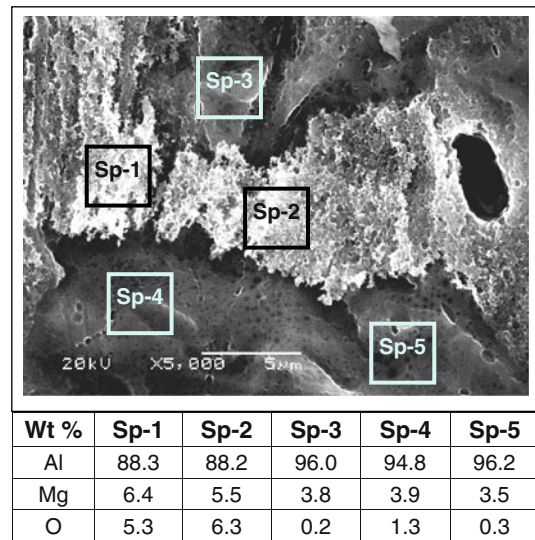
Fig. 6 Surface morphology of as-received AA5182 showing non-uniform surface oxide layer

non-uniform spots on the surface of AA5182 confirmed their high Mg and O contents (Fig. 7). While performing the analysis on the same surface in the same condition, the difference in oxygen intensities was large enough to indicate that those bright spots on the aluminum worksheet surface had higher amounts of oxygen and suggested the formation of an MgO oxide which made the oxide layer of AA5182 non-uniform in terms of composition. These results provided direct evidence for the schematic representation proposed by Kucza et al. (Ref 15) for the surface oxide layer of AA5182. These observations clearly suggested that some of the Mg particles at the surface segregated from the bulk of the surface material and produced some locally Mg- and O-rich spots, and hence made the surface oxide layer non-uniform in terms of its composition.

4.3 Effect of Grinding/Abrading on the Surface Oxide Layer

The assumption that the as-received surface would have a relatively thick and non-uniform oxide layer compared with surfaces subjected to grinding or abrading was further supported by both the general surface appearance and the chemical analysis of these surfaces. Optical microscopy of these surfaces confirmed that grinding and abrading of the sheet surface almost removed (or reduced the size) the Mg- and O-rich spots from the as-received surface (Fig. 8). Chemical analysis of some of those spots on the as-received surface confirmed the presence of high amounts of Mg and O. It was also observed that those Mg- and O-rich spots were not uniformly distributed on the entire area of as-received surface, and some areas on the surface had fewer spots than others; an area of more visible Mg- and O-rich spot is presented here. The maximum size of the Mg- and O-rich spots on the as-received surface was about in the range of 30 μm. Although on the surfaces subjected to grinding and abrading, those Mg- and O- rich spots were not very visible as compared with as-received surface, they were visible at some places in the range of 3-5 μm. Chemical analysis of these surfaces revealed that the as-received surfaces had higher amounts of oxygen than the surfaces subjected to grinding or abrading, where the intensities of aluminum on the as-received surfaces were the lowest (Fig. 9). Since oxygen was
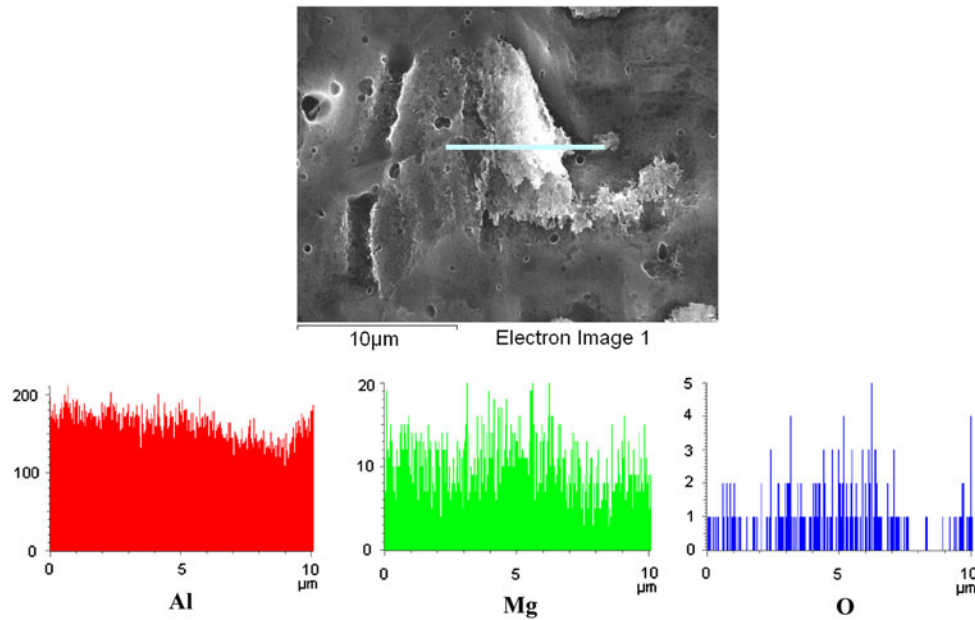
Fig. 7 Line scan chemical analysis (EDX) of non-uniform spots showing intensities of aluminum (Al), magnesium (Mg), and oxygen (O)
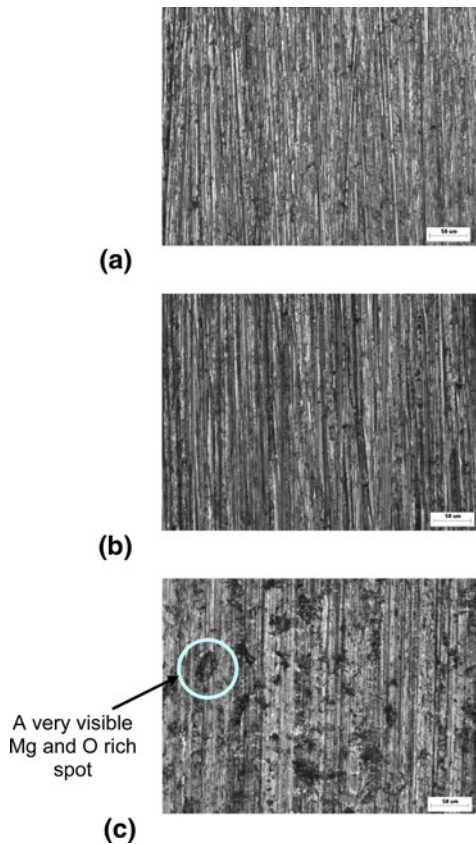
Fig. 8 Effect of grinding and abrading on the surface oxide layer of AA5182: (a) Grinding with 600 silicon carbide emery paper, (b) abrading with a scotch-brite wheel, and (c) as-received

Fig. 9 Chemical analysis of as-received, ground, and abraded surfaces of AA5182

not an alloying element of AA5182, it was likely to have come from the environment during the formation of surface oxides. The high amount of oxygen in the surface layer of as-received surface clearly indicated the presence of a thicker

and concentrated oxide layer on this surface compared with the surfaces subjected to grinding and abrading. In line with other study (Ref 5), it was also observed that the amount of magnesium was little lower on the surfaces subjected to grinding or abrading (about 4.4% compared with 4.7% on the as-received surface as shown in Fig. 9) than on the as-received surface. Although this difference was not very significant, a slightly lower value of magnesium on the surfaces subjected to grinding or abrading was likely to have been caused by the removal of Mg-rich spots from these surfaces.

4.4 Effect of Oxide Layer on Electrode Pitting and Weld Strength

The observation that the as-received surface of AA5182, in addition to alumina (Al_2O_3), had some Mg- and O-rich spots, strongly suggests the formation of MgO that were scattered over the surface. These spots were very small and covered only a small fraction of the surface. Both these oxides (Al_2O_3 and MgO) are ceramics (Ref 16) and as such they are electrical

insulators. Both these oxides (Al_2O_3 and MgO) were known to have effect on RSW of aluminum alloys in terms of electrode life and weld shear strength (Ref 14, 23, 24). It was very likely that due to the presence of a fresh and rather uniform oxide layer on the abraded sheet surface, the electrode subjected to this surface showed slower pitting compared with the electrode subjected to as-received surface which had thick and complex oxide layer. This observation was quite consistent with the suggested electrode pitting mechanism for thick and thin oxide layer of aluminum surface (Ref 14). Also, in terms of weld joint strength, although the weld shear strength of as-received surface was initially a littlie higher than that of abraded surfaces, it deteriorate quickly and the two values became almost equal at the end of 100 spot welds. In line with other study (Ref 24), this was very likely due to the presence of more MgO on the electrode face subjected to as-received surface than that of abraded surface.

5. Conclusions

The RSW of aluminum alloy 5182 with spherical tip electrodes was investigated. The influences of surface roughness and oxide layer on the electrical contact resistance of E/W interface, and the resulting electrode pitting behavior was discussed. The major findings of this study are summarized as follows:

1. The nature of oxide layer and worksheet surface roughness had influence on the electrical contact resistance of the E/W interface. However, the effect of oxide layer was dominant as all the treated worksheet surfaces, irrespective of their roughness levels, showed lower electrical contact resistance at the E/W interface than that of as-received surface.
2. Extensive plastic deformation of the worksheet surface associated with the E/W interface was believed to occur during RSW process thus suggesting that the link between the electrical contact resistance and surface roughness was likely to be related to how the oxide layer would deform during the loading.
3. Grinding and scratching of the as-received worksheet surface removed and/or reduced the size of Mg-rich spots and made the oxide layer thin and uniform. This reduced thickness of the freshly reformed oxide layer on the ground and abraded surfaces was believed to be the main reason for the low contact resistances of these surfaces compared with that of the as-received surface.
4. High heat generation and faster pitting rate due to high electrical contact resistance associated with the as-received worksheet surface was expected and observed. This finding suggested that, for AA5182, the electrical contact resistance measured before any welding (static resistance) can be used as an indicator of actual resistance spot welding behavior.

References

1. I.N. Fridlyander, V.G. Sister, O.E. Grushko, V.V. Berstenev, L.M. Sheveleva, and L.A. Ivanova, Aluminum Alloys: Promising Materials in the Automotive Industry, *Metal Sci. Heat Treat.*, 2002, **44**(9), p 365–370
2. B. Irving, Building Tomorrow's Automobiles, *Weld. J.*, 1995, **74**(8), p 29–34
3. J.A. Khan, L. Xu, and Y.J. Chao, Prediction of Nugget Development During Resistance Spot Welding Using Coupled Thermal-Electrical-Mechanical Model, *Sci. Technol. Weld. Join.*, 1999, **4**(4), p 331–336
4. I. Lum, S. Fukumoto, E. Biro, D.R. Boomer, and Y. Zhou, Electrode Pitting in Resistance Spot Welding of Aluminum Alloy 5182, *Metall. Mater. Trans. A*, 2004, **35A**, p 217–225
5. M. Rashid, S. Fukumoto, J.B. Medley, J. Villafuerte, and Y. Zhou, Influence of Lubricant on Electrode Life in Resistance Spot Welding of Aluminum Alloys, *Weld. J. Res. Suppl.*, 2007, **86**(3), p 62s–70s
6. E.P. Patrick and D.J. Spinella, The Effects of Surface Characteristics on the Resistance Spot Weldability of Aluminum Sheet, *Sheet Metal Welding Conference VII* (Detroit, MI, USA), AWS, 1996, Paper-B4
7. J. Peng, S. Fukumoto, L. Brown, and Y. Zhou, Image Analysis of Electrode Degradation in Resistance Spot Welding of Aluminum, *Sci. Technol. Weld. Join.*, 2004, **9**(4), p 331–336
8. P.S. James, H.W. Chandler, J.T. Evans, J. Wen, D.J. Browne, and C.J. Newton, The Effect of Mechanical Loading on the Contact Resistance of Coated Aluminum, *Mater. Sci. Eng. A*, 1997, **230**, p 194–201
9. M. Rashid, J.B. Medley, and Y. Zhou, Electrode Worksheet Interface Behaviour During Resistance Spot Welding of Al Alloy 5182, *Sci. Technol. Weld. Join.*, 2009, **14**(4), p 295–304
10. A. De and M.P. Theddeus, Finite Element Analysis of Resistance Spot Welding in Aluminum Alloys, *Sci. Technol. Weld. Join.*, 2002, **7**(2), p 111–118
11. M. Rashid, "Some Influences of Tribology in Resistance Spot Welding of Aluminum Alloys," Ph.D. thesis, University of Waterloo, Canada, 2007
12. E. Crinon and J.T. Evans, The Effect of Surface Roughness, Oxide Film Thickness and Interfacial Sliding on the Electrical Contact Resistance of Aluminum, *Mater. Sci. Eng. A*, 1998, **242**, p 121–128
13. P.H. Thornton, A.R. Krause, and R.G. Davies, Contact Resistance of Aluminum, *Weld. J. Res. Suppl.*, 1997, **76**(8), p 331s–341s
14. E.P. Patrick, J.R. Auhl, and T.S. Sun, *Understanding the Process Mechanism is Key to Reliable Resistance Spot Welding Aluminum Autobody Components*, SAE-Technical Paper No. 840291, SAE, Warrendale, PA, 1984
15. J.C. Kucza, J.R. Butrulle, and E. Hank, *Aluminum as Rolled Sheet for Automotive Applications—Effect of Surface Oxide on Resistance Spot Welding and Adhesive Bonding Behaviour*, SAE-Technical Paper No. 970013, SAE, Warrendale, PA, 1997
16. Ceramic and Glasses, *Engineering Materials Handbook*, Vol 4, ASM International, USA, 1991
17. H.A. Mohamed and J. Washburn, Mechanics of Solid State Pressure Welding, *Weld. J. Res. Suppl.*, 1975, **54**(9), p 302s–310s
18. U.D. Mallya, Effect of Contact Resistance in Resistance Welding of Aluminum, *Weld. J.*, 1984, **63**(2), p 41–44
19. F.J. Studer, Contact Resistance in Spot Welding, *Weld. J. Res. Suppl.*, 1939, **18**(10), p 374s–380s
20. D. Giroux and F.D. James, *Resistance Welding Manual*, 4th ed., RWMA, Philadelphia, PA, 2003
21. J.A. William, *Engineering Tribology*, Oxford University Press, UK, 1994
22. United State Military Specifications, Resistance Welding—Spot and Seam, MIL-W-6858D, 1978
23. C. Lea and J. Ball, The Oxidation of Rolled and Heat Treated Al-Mg Alloy, *Appl. Surf. Sci.*, 1984, **17**, p 344–362
24. R. Ikeda, K. Yasuda, and K. Hashiguchi, Resistance Spot Weldability and Electrode Wear Characteristics of Aluminum Alloy Sheet, *Weld. World*, 1998, **41**, p 492–498